ACS Sustainable Chemistry & Engineering

Research Article

pubs.acs.org/journal/ascecg

Gluten Biopolymer and Nanoclay-Derived Structures in Wheat Gluten–Urea–Clay Composites: Relation to Barrier and Mechanical Properties

Ramune Kuktaite,*[,†] Hasan Türe,[‡] Mikael S. Hedenqvist,[‡] Mikael Gällstedt,[§] and Tomás S. Plivelic[∥]

[†]Department of Plant Breeding, The Swedish University of Agricultural Sciences, SE-230 53 Alnarp, Sweden

[‡]School of Chemical Science and Engineering, Department of Fibre and Polymer Technology, KTH Royal Institute of Technology, SE-100 44 Stockholm, Sweden

[§]Innventia AB, P.O. Box 5604, 11486 Stockholm, Sweden

[∥]MAX IV Laboratory, Lund University, P.O. Box 118, SE-221 00 Lund, Sweden

Supporting Information

ABSTRACT: Here, we investigated the structure of natural montmorillonite (MMT) and modified Cloisite C15A (MMT pre-intercalated with a dimethyl-dehydrogenated tallow quaternary ammonium surfactant) nanoclays in the wheat gluten–urea matrix in order to obtain a nanocomposite with improved barrier and mechanical properties. Small-angle X-ray scattering indicated that the characteristic hexagonal closed packed structure of the wheat gluten–urea matrix was not found in the C15A system and existed only in the 3 and 5 wt % MMT composites. SAXS/WAXS, TGA, and water vapor/oxygen barrier properties indicated that the dispersion of the C15A clay was somewhat better than the natural MMT clay. Confocal laser scanning microscopy showed MMT clay clusters and C15A clay particles dispersed in the protein matrix, and these were preferentially oriented in the extrusion direction only at 5 wt % of the C15 clay. The water vapor/oxygen barrier properties were improved with the presence of clay. Independent of the clay content used, the stiffness decreased and the extensibility increased in the presence of C15A due to the surfactant induced changes on the protein. The opposite "more expected" clay effect (increasing stiffness and decreasing extensibility) was observed for the MMT composites.

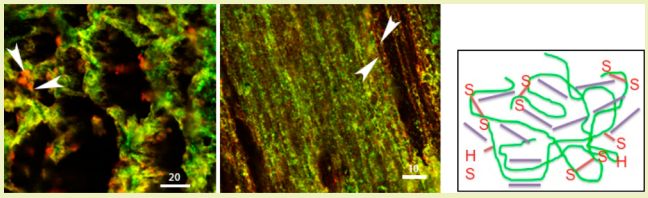

KEYWORDS: *Protein-based materials, Natural clay, Modified clay, Protein structure, Barrier and mechanical properties*

INTRODUCTION

The interest in renewable biobased materials containing nanoparticles, such as clays, is rapidly increasing.[1−3] The wheat gluten (WG) protein, a coproduct from the bioethanol and starch industries, has shown the unique and unusual properties of viscosity and elasticity[4] and has been successfully used to produce biobased plastics with intriguing properties.[5] WG in combination with chemical additives and natural nanoclays has been used for developing packaging materials and coatings.[6,7] From the chemical additives tested, urea and glycerol were found very promising in terms of a fast solvent-free production process, which is of great commercial interest.[8,9] Nanoclays, such as natural sodium-rich montmorillonite (MMT) and montmorillonite modified organically with quaternary alkylamonium, have been blended into various materials.[10] Sodium-rich montmorillonite has been tested in biobased composites, including those with WG polymer as the matrix, with the purpose to improve stiffness, oxygen and water vapor barrier, and thermal stability.[11]

Mechanical and functional properties of biobased materials are inherently linked to the material structure on a nanoscale. In WG-based materials plasticized with glycerol and containing chemical additives, such as NH_4OH and urea, a hierarchical molecular structure of hexagonally closed packed (HCP) protein objects was observed, and this structure had an impact on the WG materials properties.[12,13] WG protein components, such as monomeric gliadins and polymeric high-molecular weight glutenins (HMW-GS), are known to form specific secondary structures (α-helices, β-sheets, β-turns, etc.) under different processing conditions.[5,14,15] In WG–glycerol–urea (WGG–urea) films, the secondary protein structures as well as the HCP structures are affected significantly by the urea concentration.[13] Despite that some information on the structure of the WGG–urea–natural clay composites has been obtained previously,[16] none of the molecular stuctures and nanostructures of the WG–additive–clay composites have so far been investigated. This knowledge is essential for modeling structure–function relationships of materials and for tailoring biocomposites with specific end uses.

Received: January 10, 2014
Revised: April 23, 2014
Published: May 10, 2014

Table 1. Barrier Properties of WG Films Containing Various Amounts of Nanoclays[a]

clay concentration (wt %)	sWVTR (g mm m^{-2} day^{-1})	OP (cm^3 mm m^{-2} day^{-1} atm^{-1})
0	31.5 ± 1.6	10.4 ± 1.1
1	28.1 ± 0.8 (32.1 ± 1.5)	10.9 ± 0.1 (8.8 ± 0.6)
3	23.5 ± 0.2 (25.2 ± 2.7)	9.6 ± 0.1 (8.4 ± 1.4)
5	22.0 ± 0.9 (24.3 ± 1.9)	6.0 ± 0.4 (5.5 ± 0.3)

[a]Values outside and inside parentheses refer, respectively, to samples containing C15A and MMT clay; the latter data obtained from ref 16. ± values are standard deviations.

The aim of this work was to study the structure of the WG–urea–nanoclay composites using two types of nanoclays, natural MMT and modified C15A. The materials were studied using small-angle X-ray scattering (SAXS), wide-angle X-ray scattering (WAXS), and confocal laser scanning microscopy (CLSM), and the structural results were compared in relation to mechanical, thermal, and water vapor/oxygen barrier properties.

EXPERIMENTAL SECTION

Materials. Commercial WG powder provided by Lantmännen Reppe (Lidköping, Sweden) contained 77.7% protein (NMKL Kjeldahl; N × 5.7), 5.8% starch (Ewers polarimetric method), and 6.9% of moisture (NMKL method no. 23). Glycerol (≥99.5 wt %) was provided by Tefac (Karlshamn, Sweden), and urea (≥99.5 wt %) was purchased from Merck (Darmstadt, Germany). Cloisite Na^+ (natural sodium-rich montmorillonite; CNa) and Cloisite 15A (modified sodium-rich montmorillonite; C15A) clays were obtained from Southern Clay Products, Inc. (U.S.A.). C15A is a natural clay modified with a dimethyl-dehydrogenated tallow quaternary ammonium compound (2M2HT), where the dihydrogenated tallow consists of C18 ∼65%; C16 ∼30%; C14 ∼5%, and Cl is the counterion.

Preparation of Composites. The moisture content of the WG powder was adjusted to about 6 wt % before extrusion. Nanocomposites were prepared from WG and clays by first dry-mixing and shaking the components for 5 min at room temperature as described in Türe et al.[16] Urea was blended into the mixture, and 30% glycerol (with respect to WG and glycerol content) was added using a food mixer WATT (Duka AB, Sweden) at 150 rpm for 10 min. The amount of clays was 1, 3, and 5 wt % with respect to the weight of WG and glycerol (70/30), and 10 wt % of urea was added (relative to the total weight of the prepared blend). Samples were designated as WGG-10U-1Na for 1 wt % of MMT and WGG-10U-1C15A for 1 wt % of modified MMT. The extrusion was performed using a single-screw extruder (BX18, Axon, Sweden) as described in Türe et al.,[16] and extruded samples were stored at −25 °C temperature.

X-ray Scattering. Small-angle X-ray scattering (SAXS) measurements were performed at the beamline I911-4, at the MAX IV Laboratory Synchrotron, Lund University, Sweden.[17] A monochromatic beam with a wavelength (λ) of 0.91 Å was used, and two sample–detector distances, 1324.9 and 1906.5 mm, were employed to cover the scattering vector q range of 0.08–7 nm^{-1} (where $q = (4\pi/\lambda)\sin\theta$, and 2θ is the scattering angle). Two dimensional scattering pattern was obtained using Pilatus 1M detector (Dectris) with an exposure time of 5 min. The data were azimuthally averaged, normalized by the integrated incident intensity, and corrected for background scattering using the bli911-4 software.[17]

Wide-angle X-ray scattering (WAXS) was performed at the beamline 911-5 of the same synchrotron.[18] The wavelength of 0.907 Å was used, and the sample–detector distance was 150.6 mm. Two-dimensional images were recorded using a CCD detector (model Marresearch, GmbH) with an exposure time of 3 min. The data were processed using the FIT2D software.[19]

Confocal Laser Scanning Microscopy (CLSM). The high molecular weight glutenin subunits (HMW-gs) 2, 5, 10, 12 in the WGG–urea–clay composites were immunolabeled with the monoclonal and gliadins with the polyclonal primary antibodies[12] in the WGG–urea–clay composites. Washed samples were incubated with two secondary antibodies, Alexa 488 and Alexa 546 (Molecular Probes, Eugene, Oregon, U.S.A.), washed, and viewed using CLSM.

Thermogravimetric Analysis (TGA). The thermogravimetric measurements were carried out in a Mettler Toledo TGA/SDTA 851 by heating approximately 5 mg of the samples in 70 μL open alumina pans from 40 to 800 °C at a heating rate of 10 °C min^{-1} in air.

Porosimetry. A Micromeritics ASAP 2000 porosimetry system was used to obtain the surface area. The samples were evacuated at 110 °C, and the analyses were run at liquid nitrogen temperature.

Oxygen Permeability (OP). The oxygen transmission rate was determined in accordance with ASTM D 3985-95 at 23 °C and 50% RH using a Mocon Ox-Tran 2/20 from Modern Controls, Inc., MN, U.S.A. One side of the sample was exposed to flowing oxygen (99.95%) at atmospheric pressure. The oxygen transmission rate was normalized with respect to the oxygen pressure and film thickness to yield oxygen permeability (OP). Two replicates from each sample were used. The full procedure is given in Türe et al.[16]

Water Vapor Transmission Rate (WVTR). The water vapor transmission rate was measured on two replicates of each sample using a Mocon Permatran-W 3/31 according to ASTM F 1249-90 at 23 °C with a 50–0% RH gradient across the film sample. The WVTR was normalized with respect to the film thickness giving the specific water vapor transmission rate (sWVTR). The full procedure is given in Türe et al.[16]

Moisture Content. Circular samples (diameter = 20 mm) were preconditioned at 23 °C and 50% RH for one week. After being weighed (the initial weight), samples were dried in a desiccator containing silica gel powders for one week at room temperature. The moisture content (%) was calculated as the difference in weight between the initial and the dry state relative to the initial weight. All the measurements were performed on five replicates.

Tensile Testing. Mechanical properties of the dumb-bell samples were measured according to ISO 527-37/120 using an Instron 5566 tensile tester (Instron Corp. Ltd., MN, U.S.A.) with a 100 N load cell, using a crosshead speed of 100 mm/min. Dumb-bell shaped specimens, with a length and width of the narrow section of, respectively, 16 ± 1.0 and 4 ± 1.0 mm (ISO 37:1994) were punched out from films along the extrusion direction and tested at 23 °C and 50% RH. Specimens were conditioned for one week at 23 °C and 50% RH before tensile testing.

RESULTS AND DISCUSSION

Barrier Properties. Table 1 presents the permeability data of the samples with different contents of modified C15A. In Table 1, for a comparison, results from similar samples with unmodified MMT clay were also included. With the addition of 5 wt % C15A, the sWVTR and OP values were 70% and 58%, respectively, of the values of the clay-free sample. Noteworthy is that both the decrease in sWVTR and OP were in most cases the same for the modified and unmodified clay composites. Using TGA, it was found that C15A contained 57 wt % clay, with the rest being the surfactant. In volume terms, the amount of clay was even lower (assuming that the density of the clay is higher than that of the surfactant). Hence, if the two systems experience the same degree of clay dispersion, it would be expected that the natural MMT system would have a better gas barrier than the C15A system due to the larger amount of clay

Table 2. Mechanical Properties of WG Films Containing Various Amounts of Nanoclays[a]

clay concentration (wt %)	moisture content (%)	elastic modulus (MPa)	maximum stress (MPa)	strain at maximum stress (%)
0	10.6 ± 0.8	7.3 ± 0.9	3.4 ± 0.5	72.7 ± 7.2
1	10.2 ± 0.3 (10.5 ± 0.2)	4.9 ± 0.7 (7.2 ± 0.9)	2.6 ± 0.4 (3.7 ± 0.5)	115.8 ± 22.8 (98.4 ± 21.6)
3	9.7 ± 0.5 (10.3 ± 0.3)	5.7 ± 0.7 (9.3 ± 0.5)	2.5 ± 0.3 (3.6 ± 0.6)	89.6 ± 21.2 (80.7 ± 18.9)
5	9.8 ± 0.2 (10.0 ± 0.5)	6.1 ± 0.5 (11.2 ± 1)	2.9 ± 0.5 (3.2 ± 0.4)	94.2 ± 21.6 (58.8 ± 11.7)

[a]Values outside and inside parentheses refer, respectively, to samples containing C15A and MMT clay; the latter data obtained from ref 16. ± values are standard deviations.

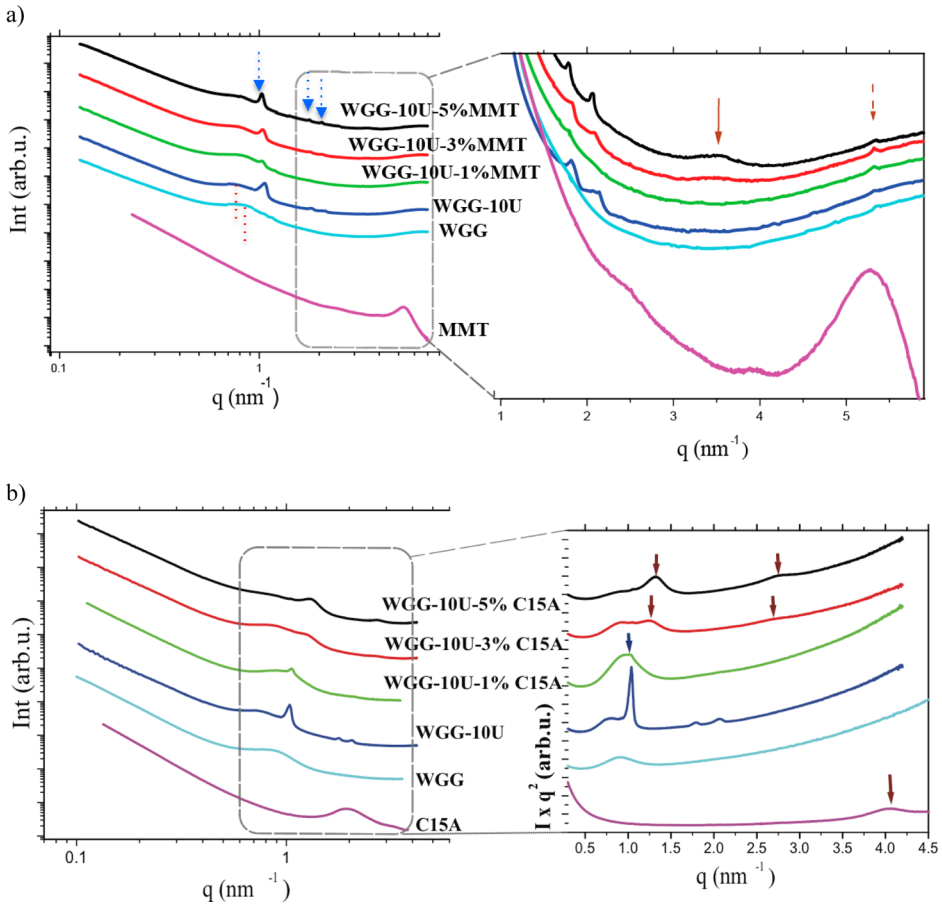

Figure 1. SAXS patterns of WGG-10U samples: (a) MMT; red dashed line (a broad peak). Blue arrows are the Bragg's peaks positions of the HCP structure. In the magnified part, the red arrows indicate peaks of the clay layers stacking. (b) C15A; In the magnified part, the blue arrow in the 1 wt % C15A sample indicates the Bragg's peak from the HCP structure. Dark red arrows indicate the clay layers stacking in C15A powder and organized structures of the organically modified clay and protein molecules.

platelets in the MMT composites. It is here assumed that the surfactant does not contribute to any barrier improvement relative to the wheat gluten matrix. Whereas the OP is probably not reduced in the presence of the surfactant, it may still have an effect on the water uptake, because of the fatty acid tails, and hence the water barrier. However, as observed in Table 2, the moisture content was, within the standard deviation, the same and independent of the clay type and content. Hence, the effect of the surfactant also on the water barrier was considered to be small. As previously shown, the natural MMT/wheat gluten system contains both intercalated and exfoliated clay, as well as large protein aggregates.[16] Because the same improvement in barrier properties was achieved with C15A with a clay platelet content slightly more than half of that of the MMT system, it is suggested that the degree of clay dispersion was better in the former case.

Mechanical Properties. The mechanical properties of the C15A composites are presented in Table 2 (values for the MMT composites are presented as a comparison). The modulus increased with the addition of MMT (Table 2). For C15A, however, the modulus decreased in the presence of clay. The theoretical moduli for the 5 wt % MMT and C15A composites were calculated. Assuming a density of MMT, WG, and 2M2HT of, respectively, 2608,[20] 1300,[21] and 870[22] kg/m^3, the volume fractions were obtained and enabled the composite moduli to be calculated. The upper ($E = \sum_i \nu_i E_i$) and lower ($1/E = \sum_i \nu_i/E_i$) bound equations were used; ν_i and E_i refer to the volume fraction and modulus of the MMT, WG, and 2M2HT components, respectively. The modulus of 2M2HT was taken to be the same as WG (Table 2), and the tensile modulus for MMT (11 GPa) was calculated from the bulk (11 GPa) and shear (5.5 GPa) moduli.[23] The calculated upper and lower bound composite tensile moduli for 5 wt % MMT were 289

dx.doi.org/10.1021/sc500017y | ACS Sustainable Chem. Eng. 2014, 2, 1439−1445

Table 3. Morphological Distances of WGG-10U Films Containing Various Amounts of MMT and C15A Clays

	morphological distances d (Å)			
	protein		clay	
sample name	d (broad peak WGG)	d_I (HCP)	d_{clay}	d_{clay}
WGG	74.8	–	–	–
WGG-10U	84.9	68.4	–	–
MMT powder	–	–	–	11.8
WGG-10U-1%MMT	78.9	70.5	18.8	11.8
VVGG-10U-3%MMT	80.4	69.9	17.7	11.8
WGG-10U-5%MMT	79.8	70.5	17.7	11.8
C15A powder	–	–	32.3	18.8
WGG-10U-1%C15A	67.6	70.9	60.0	n.o.[a]
WGG-10U-3%C15A	67.5	69.2	50.0	23.2
WGG-10U-5%C15A	71.1	68.3	47.6	22.7

[a]n.o. - not observed.

and 7.5 MPa, respectively. The measured modulus was only slightly higher than the lower bound. The corresponding values for C15A were 165 and 7.4 MPa. The measured value (Table 2) was slightly lower than the lower bound. For most cases, the maximum stress was independent of the clay content. The average values of the C15A composites were, however, consistently lower than those of the clay-free sample and the MMT composites. The extensibility (strain at maximum stress) was consistently higher for the C15A system as compared to the MMT system. In fact, both types of clay composites (with one exception) had higher extensibility than the clay-free sample. For the composites that experienced both a lower modulus and a higher extensibility in the presence of clay (C15A), the surfactant seemed to act as a plasticiser in the wheat gluten−urea system. The observed results could be partly explained by considering the results on injection molded wheat gluten containing MMT[6] and C15A (Tables S1−S3, Supporting Information). Even though the shearing effects, process temperatures, and recipes were different from the present extrusion work, a comparison of the effects of the two clays with the injection-molded wheat gluten system is possible and meaningful.

Indeed, as in the present system, the presence of natural MMT increased the modulus, while the presence of C15A had an opposite effect. At the same time, a small decrease in the glass transition was noted for the MMT composites, while a greater decrease was observed in the presence of C15A. The small decrease in T_g in the presence of MMT was difficult to explain; however, the decrease in T_g in the C15A system can partly be explained by protein solubility data (not shown). It was observed that in the presence of C15A the protein solubility due to the disruption of secondary bonds/and disulphide bonds (using sodium dodecyl sulfate and sonication) was significantly greater than in the clay-free and MMT containing samples. To conclude, the plasticization effects observed here in the presence of the surfactant was not directly due to the dimethyl-dihydrogenated tallow quaternary ammonium chloride surfactant itself (the content was too small) but due to its physicochemical effects on the gluten protein (protein depolymerisation and reduced aggregation). It is also possible that interactions between the surfactant and urea amplified this effect.[24] Interestingly, combining a surfactant having these properties with impermeable clay yields a plasticization combined with improved barrier properties. Generally, when a plasticizer is added to a polymer the barrier properties become poorer. The natural clay, on the other hand, increased the protein polymerization and aggregation.[6] Hence, these properties together with the reinforcement due to the clay itself led to a classical increase in both stiffness and barrier properties.

SAXS of Wheat Gluten−Urea−Clay Composites and Porosimetry of Clay Powders. The SAXS curves with characteristic distances of the WGG-10U films, containing 1, 3, and 5 wt % MMT or C15A, are presented in Figure 1 and Table 3. The SAXS curves for WGG and WGG-10U indicated a broad peak at 74.8 Å (q = 0.84 nm^{-1}) and 84.9 Å (q = 0.74 nm^{-1}) (Figure 1a, dashed red lines). The larger distance observed for the WGG-10U compared to WGG seemed to be a result of urea-induced swelling. For the WGG-10U films, three Bragg peaks with a positional ratio of 1:$3^{1/2}$:$4^{1/2}$ were observed (Figure 1a; blue arrows). The three peaks indicated a hexagonal close packed (HCP) structure with an interdomain distance d_I of 68.4 Å (where $d_I = 4\pi/(3)^{1/2}q_1$, and q_1 is the position of the maxima of the first Bragg peak), similar to what was also observed in the WGG−urea films.[13] The HCP structure has been observed nearly in all MMT samples [although, for 1 wt % MMT, the two small peaks (high order reflections of the HCP) were not well developed or were absent], showing the same d_I distance (Table 3).

This indicates no clay effect on the HCP structure at 3 and 5 wt % MMT, while for 1 wt % MMT, a small decrease in intensity of the first Bragg peak (and absence of the two small Bragg peaks) is possibly due to an optimum ratio (more uniform dispersion) between the WG polymer domains and negatively charged MMT galleries,[25] which influence the HCP formation.

For 1 wt % MMT, the (001) d-spacing of the clay peak, d_{clay}, (average distance between the silicate layers) was equal to 18.8 Å and shifted toward a lower d_{clay} value of 17.7 Å at 3 and 5 wt % MMT (Figure 1a, solid red arrow). The increase in d-spacing compared to the pristine MMT of 11.8 Å indicated the WG polymer inside the clay galleries, for example, intercalated morphology (Figure 1a, dashed red arrow).

The small MMT peak with a d_{clay} value of 11.8 Å in all the WGG-10U-MMT samples suggests that not all clays were intercalated/exfoliated; for example, some of the clay remained unaffected with the same d_{clay} as pristine MMT (Figure 1a, dashed red arrow in the magnified part). Hence, the WGG samples at all the MMT concentrations tested demonstrated a certain extent of clay intercalation, which was also observed earlier, together with exfoliated clay and larger agglomerates.[16]

For the WGG-10U-C15A composites, SAXS curves showed a broad undeveloped shoulder at 67.6 Å (q = 0.93 nm^{-1}) for 1 and 3 wt % C15A, with the greater distance of 71.1 Å (q = 0.88 nm^{-1}) for 5 wt % C15A (Figure 1b; Table 2). With increasing C15A clay concentration, a decreasing HCP distance d_1 equal to 70.9 Å (q = 0.102 nm^{-1}), 69.2 Å (q = 0.104 nm^{-1}), and 68.34 Å (q = 0.106 nm^{-1}) was observed (Table 3). Important to note is that the sharp Bragg peak (in the WGG-10U sample) from the HCP structure was observed in the 1 wt % C15A sample (indicated by blue arrow, in Figure 2b, magnified part), while

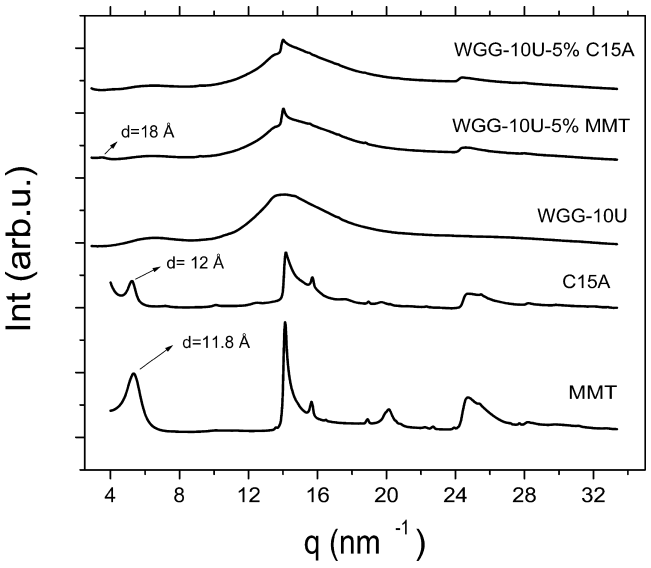

Figure 2. WAXS patterns of WGG-10U samples with C15A and MMT clays, WGG-10U control, and natural MMT and C15A pure clay powders.

no HCP structure peaks (except the very small first Bragg peak) were observed for 3 and 5 wt % C15A samples (Figure S1, Supporting Information). This indicated that no HCP structure was observed in the C15A system. A decrease in the d_{clay} distances for the 1, 3, and 5 wt % C15A samples was observed, resulting in distances 60.0, 50.0, and 47.6 Å, respectively (Figure 1b). d_{clay} spacings between 28 and 34 Å have been reported for C15A clay.[26,27] Here, we suppose that these much larger distances may be attributed to the intercalation of the clay between the WG polymer domains.

The first broad peak in the SAXS curves of the C15A samples seemed to originate from the peaks of WGG-10U and the first reflection of the intercalated clay structure; the major part of the clay peak shifted toward the WGG peak for the 3 and 5 wt % C15A samples (Figure 1b, first red arrow in the magnified part). At 3 and 5 wt % C15A, possible intercalation distances between clay platelets for the second peak were 23.2 Å (q = 0.271 nm^{-1}) and 22.7 Å (q = 0.277 nm^{-1}), respectively (Figure 1b; Table 3). To conclude, the C15A composites showed two peaks of intercalated clay with a distance d_{clay} shifting toward greater values with lower amounts of clay (lower q). This indicated that the WG polymer was presented in the clay-stacked structure at all clay concentrations (1, 3, and 5 wt %) (Figure 1b).

SAXS curves of clay powders showed one broad peak at d_{clay}= 11.8 Å for the natural MMT clay, and two broad peaks for the modified C15A clay, with d_{clay}-spacings of 32.3 and 18.8 Å, respectively (Figure 1a,b). The difference in the basal spacing d_{001} between the studied clays was due to the Na^+ ions being replaced by the larger organic modifiers in the C15A clay.[28]

In this study, the C15A clay seemed to have a significant effect on the WG polymer, which was favored due to the presence of urea, which is known to denaturate and open or unfold the protein.[29]

Findings in this study on the C15A clay exfoliation/interaction in the protein matrix are in accordance with similar studies on WG and modified Cloisite-30B.[30] It is not unreasonable to assume that the pre-intercalation using the surfactant facilitated the dispersion of the clay in the protein. The BET surface area of the two clay powders was measured. The values of MMT and C15A were, respectively, 17.5 and 6.7 m^2/g. These were considerably lower than that of individual clay layers (on the order of 500−800 m^2/g), which was explained by the fact that the liquid nitrogen used in the analysis does not penetrate the clay interlayers.[31] It is interesting to note here that this was also the case for the pre-intercalated clay (C15A). The smaller "available" area of C15A suggested that it would be more difficult to delaminate C15A than MMT. However, during extrusion, the pre-intercalated clay is probably easier to delaminate during the action of shear forces, which in this study resulted into more effective C15A and biobased polymer compatibility compared to the MMT clay−WG samples. A similar result was observed for biopolymer (e.g., poly(L-lactide)/poly(butylene succinate) and nanoclay blends and was attributed to a compatibilization effect.[32]

WAXS of Wheat Gluten−Urea−Clay Composites. Examples of WAXS curves of 5 wt %-modified C15A, natural MMT composites, and both clay powders are presented in Figure 2. For the MMT and C15A powders, the clay peaks of 11.8 and 12 Å were observed, respectively, in a good agreement with the SAXS data (Figure 2).

The scattering intensity of the studied clays corresponded to the clay concentration of the sample; for example, the greatest intensity was observed at 5 wt % WGG composites (Figure S2, Supporting Information). For the 5 wt % MMT clay composite, a peak with characteristic distance d = 18 Å was observed, indicating intercalated WGG−urea−clay morphology. The peak intensity ratio of this peak and the internal peak at q = 14 nm^{-1} was lower than the corresponding ratio of the pristine clay (d = 11.8 Å and q of ∼5.5 nm^{-1}) and the peak at q = 14 nm^{-1}, indicating a certain amount of exfoliated clay platelets (Figure 2). For the 5 wt % C15A clay sample, no such distance was observed, indicating a sizable amount of the exfoliated clay platelets (Figure 2). For all MMT and C15A composites, the observed clay peak at q of about 14 nm^{-1} confirmed that there was always clay in the beam.

Thermogravimetry. The TGA results in Figure 3 show that the residual char of the WGG sample at 800 °C was 5.3 wt %. The same value for the sample with 5 wt % MMT was 14.8 wt %. The large char residue indicated that a significant amount of WGG was located between "protective" clay sheets, which reduced the evaporation of WGG degradation products during the experiment. The amount of char in the 5 wt % C15A sample was 8.8 wt %. If this content was normalized to 5 wt % pure clay (in C15A, the amount of pure clay and surfactant was 2.85 and 2.15 wt %, respectively), the amount of char was 15.4 wt %. This amount is slightly higher than that of the MMT composite and indicated that the degree of intercalation, or protection efficiency, at the same pristine clay content was

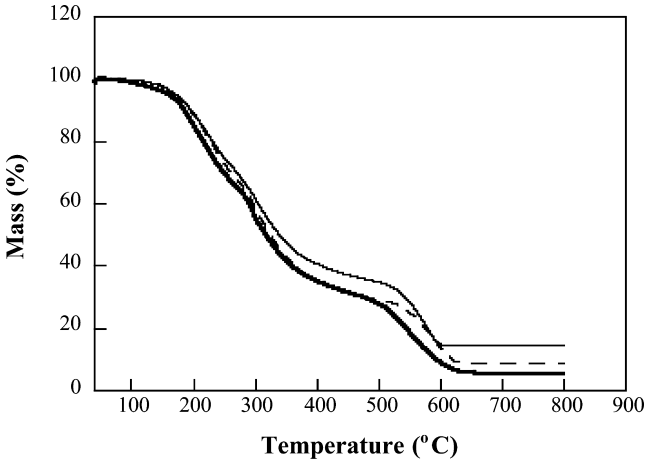

Figure 3. Mass of WGG (solid bold curve), WGG with 5 wt % MMT (solid thin curve), and WGG with 5 wt % C15A (broken curve) as a function of temperature.

similar or slightly better in the C15A sample relative to that of the MMT sample.

Confocal Laser Scanning Microscopy (CLSM). Varying microstructural morphology of natural and modified clay WGG-10U films was observed by CLSM (Figure 4). The

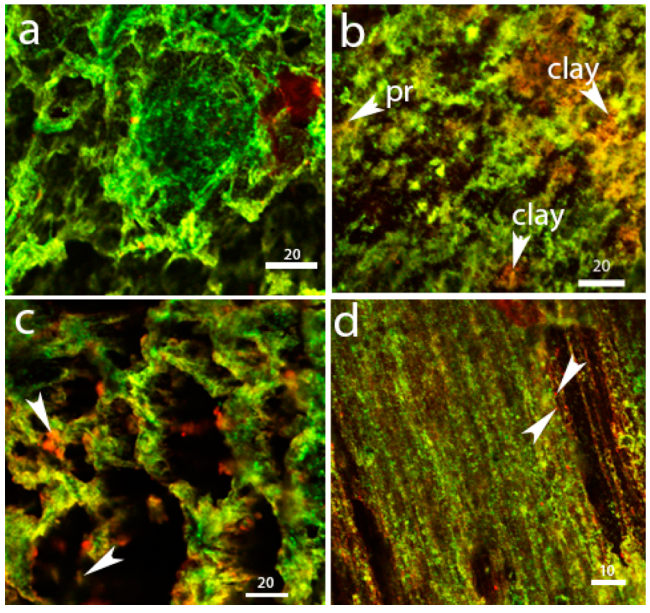

Figure 4. CLSM images of WGG samples: (a) control WGG, (b) 1wt % natural MMT, (c) 5 wt % natural MMT, and (d) 5 wt % C15A. Monoclonal HMW glutenins are green. Polyclonal gliadins and clays particles are red. In panel b, "pr" arrows indicate protein and "clay" arrows indicate C15A clay. In panel c, arrows indicate stacks. In panel d, arrows indicate dispersal in the protein matrix.

1 wt % MMT film showed areas of aggregated HMW-GS and gliadin proteins with some clay particles dispersed in the WG protein matrix (Figure 4b, clay particles indicated by arrows). These dispersed clusters of the natural clay particles were observed to be bigger at higher concentrations of natural clay (Figure 4c, shown by arrows). A totally different picture was observed for the WGG-10U containing 5 wt % C15A (Figure 4d). Proteins, such as HMW-GS and gliadins (green and red colors), seemed to form a rather homogeneous protein matrix, in which modified C15A clay nanoparticles were incorporated in a dispersed fashion. It is important to mention that a clearly uniaxial-oriented protein structure pattern was observed only for the 5 wt % C15A and not for 1 wt % C15A containing WG samples in this study (unpublished results).

CONCLUSIONS

The decrease in water vapor/oxygen barrier properties due to the presence of nanoclays was found to be similar for the unmodified MMT and modified C15A WGG−urea−clay composites. However, the mechanical properties were found to be different. For the MMT system with all the clay contents studied, the modulus increased, and the strain at break (extensibility) decreased. However, for the C15A composites, a decrease in modulus and an increase in strain at break were observed.

The HCP structure observed in clay-free WGG−urea samples[13] was found WGG−urea composites with 3 and 5 wt % MMT clay. For the C15A composites, the HCP structure was not observed. Results indicated that both the MMT and C15A composites contained intercalated and exfoliated clay. The intercalation was found to be more pronounced, i.e., larger d_{clay} values, at lower clay concentrations (1 wt % versus 3 and 5 wt %), and it was even more pronounced in C15A clay samples compared to MMT samples.

The C15A nanoclay showed a greater compatibility with the WGG protein matrix, i.e., a polymer with more uniform and less aggregated pattern of proteins, compared to the natural MMT clay composites. A schematic presentation of the WGG−urea−5 wt % C15A composite structure is shown in Scheme 1. The reason for the surfactant-induced "plasticizer" effect was suggested to be due to induced depolymerization/reduced aggregation of WG.

Scheme 1. WGG-10U Polymer Interaction with C15A Clay Nanoparticles.

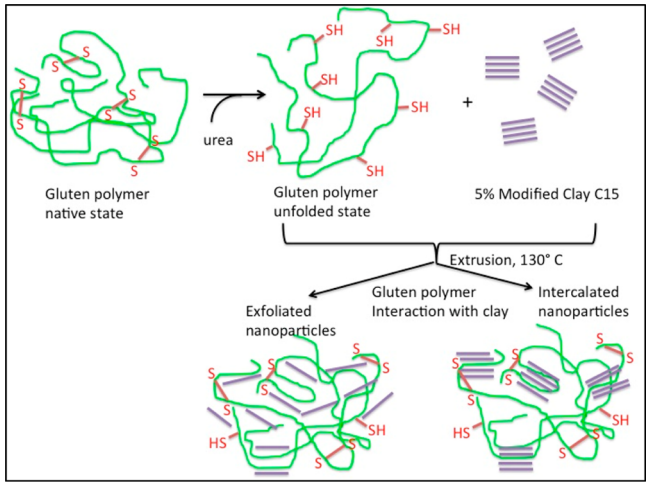

ASSOCIATED CONTENT

Supporting Information

Tensile properties of samples in transverse and radial direction, glass transition properties by DSC, SAXS patterns of C15A clay composites, and WAXS of natural MMT and C15A clay composites. This material is available free of charge via the Internet at http://pubs.acs.org.

AUTHOR INFORMATION

Corresponding Author

*E-mail: ramune.kuktaite@slu.se. Phone: +46 40 415337.

Present Address

H. Türe: Ordu University, Faculty of Marine Sciences, Department of Marine Science and Technology Engineering, 52400 Fatsa, Ordu, Turkey

Notes

The authors declare no competing financial interest.

ACKNOWLEDGMENTS

We acknowledge the financial support from the Research Program "Trees and Crops for the Future (TC4F)" in Sweden, VINNOVA, and MAX-IV Laboratory, Lund University, beamlines I711, I911-4, and I911-5 for the provision of beamtime.

REFERENCES

(1) Dean, K.; Yu, L. Biodegradable Protein−Nanoparticle Composite. In *Biodegradable Polymers*; Smith, R., Ed.; Woodhead: Cambridge, U.K., 2005.

(2) Zhu, L.; Wool, R. P. Nanoclay reinforced bio-based elastomers: Synthesis and characterization. *Polymer* **2006**, *47*, 8106−8115.

(3) Shin, Y.-J.; Song, H-Y.; Jo, W.-S.; Lee, M.-J.; Song, K. B. Physical properties of a barley protein/nano-clay composite film containing grapefruit seed extract and antimicrobial benefits for packaging of *Agaricus bisporus*. *Int. J. Food Sci. Technol.* **2013**, *48*, 1736−1743.

(4) Shewry, P. R.; Tatham, A. S. The prolamin storage proteins of cereal seeds structure and evolution. *Biochem. J.* **1990**, *267*, 1−12.

(5) Johansson, E.; Malik, A. H.; Hussain, A.; Rasheed, F.; Newson, W. R.; Plivelic, T.; Hedenqvist, M. S.; Gälstedt, M.; Kuktaite, R. Wheat gluten polymer structures: The Impact of genotype, environment and processing on their functionality in various applications. *Cereal Chem.* **2013**, *90*, 367−376.

(6) Cho, S. W.; Gällstedt, M.; Johansson, E.; Hedenqvist, M. Injection-molded composites and materials based on wheat gluten. *Int. J. Biol. Macromol.* **2011**, *48*, 146−152.

(7) Nordqvist, P.; Johansson, E.; Khabbaz, F.; Malmström, E. Characterization of hydrolysed or heat treated wheat gluten by SE-HPLC and ^{13}C NMR: Correlation with wood bonding performance. *Ind. Crop. Prod.* **2013**, *51*, 51−61.

(8) Hernandez-Izquierdo, V. M.; Krochta, J. M. Thermoplastic processing of proteins for film formation − Review. *J. Food Sci.* **2008**, *73*, 30−39.

(9) Türe, H.; Gällstedt, M.; Johansson, E.; Kuktaite, R.; Hedenqvist, M. S. Protein network structure and properties of wheat gluten extrudates using a novel solvent-free approach with urea as a combined denaturant and plasticizer. *Soft Matter* **2011**, *7*, 9416−9423.

(10) Yu, L.; Dean, H.; Li, L. Polymer blends and composites from renewable resources. *Prog. Polym. Sci.* **2006**, *31*, 576−602.

(11) Majeed, K.; Jawaid, M.; Hassan, A.; Bakar, A. A.; Khalil, H. P. S. A.; Salema, A. A.; Inuwa, I. Potential materials for food packaging from nanoclay/natural fibres filled hybrid composites. *Mater. Des.* **2013**, *46*, 391−410.

(12) Kuktaite, R.; Plivelic, T.; Cerenius, Y.; Hedenqvist, M. S.; Gällstedt, M.; Marttila, S.; Ignell, R.; Popineau, I.; Tranquet, O.; Shewry, P.; Johansson, E. Wheat gluten bio-materials structure: From polymeric protein aggregates toward hexagonal arrangements. *Biomacromolecules* **2011**, *12*, 1438−1448.

(13) Kuktaite, R.; Plivelic, T. S.; Türe, H.; Hedenqvist, M. S.; Gällstedt, M.; Marttila, S.; Johansson, E. Changes in the hierarchical protein polymer structure: Urea and temperature effects on wheat gluten films. *RSC Adv.* **2012**, *2*, 11908−11914.

(14) Kasarda, D. D.; Bernardin, J. E.; Thomas, R. S. Reversible aggregation of alpha-gliadin to fibrils. *Science* **1967**, *155*, 203−205.

(15) Shewry, P. R.; Popineau, Y.; Lafiandra, D.; Belton, P. Wheat glutenin subunits and dough elasticity: Findings of the EUROWHEAT project. *Trends Food Sci. Technol.* **2001**, *11*, 433−441.

(16) Türe, H.; Blomfeldt, T. O. J.; Gällstedt, M.; Hedenqvist, M. S. Properties of wheat-gluten/montmorillonite nanocomposite films obtained by a solvent-free extrusion process. *J. Polym. Environ.* **2012**, *20*, 1038−1045.

(17) Labrador, A. L.; Cerenius, Y.; Svensson, C.; Theodor, K.; Plivelic, T. S. The yellow mini-hutch for SAXS experiments at MAX IV Laboratory. *J. Phys. Conf. Ser.* **2013**, *425*, 072019.

(18) Mammen, C. B.; Ursby, T.; Cerenius, Y.; Thunnissen, M.; Als-Nielsen, J.; Larsen, S.; Liljas, A. L. Design of a 5 stations macromolecular crystallography beamline at MAX-lab. *Acta Phys. Pol., A* **2002**, *101*, 595−602.

(19) Hammersley, A. P.; Svensson, S. O.; Hanfland, M.; Fitch, A. N.; Hausermann, D. Two-dimensional detector software: From real detector to idealised image of two-theta scan. *High Pressure Res.* **1996**, *14*, 235−248.

(20) Grim R. E. *Clay Mineralogy*; McGraw-Hill: New York, 1968.

(21) Cho, S.-W.; Gällstedt, M.; Hedenqvist, M. S. Effects of glycerol content and film thickness on the properties of vital wheat gluten films, cast at pH 4 and 11. *J. Appl. Polym. Sci.* **2010**, *117*, 3506−3514.

(22) Santa Cruz Biotechnology. www.scbt.com.

(23) Vanorio, T.; Prasad, M.; Nur, A. Elastic properties of dry clay mineral aggregates, suspensions and sandstones. *Geophys. J. Int.* **2003**, *155*, 319−326.

(24) Keawkumai, C.; Jarukumjorn, K.; Wittayakun, J.; Suppakarn, N. Influences of surfactant content and type on physical properties of natural rubber/organoclay nanocomposites. *J. Polym. Res.* **2012**, *19*, 9917.

(25) Chen, P.; Zhang, L. Interaction and properties of highly exfoliated soy protein/montmorillonite nanocomposites. *Biomacromolecules* **2006**, *7*, 1700−1706.

(26) Pozsgay, A.; Fráter, T; Százdi, L.; Müller, P.; Sajó, I.; Pukánszky, B. Gallery structure and exfoliation of organophilized montmorillonite: Effect on composite properties. *Eur. Polym. J.* **2004**, *40*, 27−36.

(27) Ton-That, M. T.; Perrin-Sarazin, F.; Cole, K. C.; Bureau, M. N.; Denault, J. Polyolefin nanocomposites: Formulation and development. *Polym. Eng. Sci.* **2004**, *44*, 1212−1219.

(28) Okamoto, M. Precise Synthesis, Materials Properties, Applications. In *Macromolecular Engineering*; Matyjaszewski, K., Gnanou, Y., Leibler L., Eds.; Wiley-VCH Verlag: Weinheim, Germany, 2007; pp 2071−2130.

(29) Hua, L; Zhou, R.; Thirumalai, D.; Berne, B. J. Urea denaturation by stronger dispersion interactions with proteins than water implies a 2-stage unfolding. *Proc. Natl. Acad. Sci. U.S.A.* **2008**, *105*, 16928−16933.

(30) Zhang, X.; Do, M. D.; Dean, K.; Hoobin, P.; Burgar, I. M. Wheat-gluten-based natural polymer nanoparticle composites. *Biomacromolecules* **2007**, *8*, 345−353.

(31) Helmy, A. K.; Ferreiro, E. A.; de Bussetti, S. G. Surface area evaluation of montmorillonite. *J. Colloid Interface Sci.* **1999**, *210*, 167−171.

(32) Chen, G. X.; Kim, H. S.; Kim, E. S.; Yoon, J. S. Compatibilization-like effect of reactive organoclay on the poly(L-lactide)/poly(butylene succinate) blends. *Polymer* **2005**, *46*, 11829−11836.